Chapter 2
Patient-Derived Xenograft Models in Gynaecological Malignancies

Tomohito Tanaka and Masahide Ohmichi

Abstract Established suitable models are important for cancer research. The recent progression of genomic or molecular analysis and precision medicine requires cancer models that reflect the characteristics of primary tumours. Patient-derived xenograft (PDX) models have been focussed on because of their similarity between PDX and primary tumours. PDX represents a promising tool for translational research since it closely resembles patient tumour features and retains molecular and histological features. Currently, PDX has been established in several types of cancer, including colon, stomach, breast, uterine, and ovarian cancers. However, several problems still exist. This review provides information on recent methods for the implantation and analysis of tumour characteristics in gynaecological cancers.

Keywords Gynaecological malignancy · Cervical cancer · Endometrial cancer Ovarian cancer · Patient-derived xenograft

2.1 Introduction

Molecular and genomic analyses have developed remarkably during the last decade. Several cell lines have been established and used for cancer research. Authentic, established cell lines express fixed gene arrangements and act in similar molecular

T. Tanaka (✉)
Department of Obstetrics and Gynecology, Osaka Medical College, Takatsuki, Japan

Translational Research Program, Osaka Medical College, Takatsuki, Japan
e-mail: gyn123@osaka-med.ac.jp

M. Ohmichi
Department of Obstetrics and Gynecology, Osaka Medical College, Takatsuki, Japan

S. Isonishi, Y. Kikuchi (eds.), *Molecular Diagnosis and Targeting for Gynecologic Malignancy*, Current Human Cell Research and Applications,
https://doi.org/10.1007/978-981-33-6013-6_2

pathways in certain situations, which has been useful in cancer research. However, researchers require more detailed gene information in each cancer cell and should be able to reproduce the tumour microenvironment.

Patient-derived xenograft (PDX) models, which are new animal models, are established by heterotopic or orthotopic grafting of fresh surgically resected tumour tissue into immune-deficient mice. The obtained tumour tissue is washed with saline and stored in a cell culture medium on ice, to reduce tissue metabolism. The tumour tissue should be implanted into animals as soon as possible, as prolonged implantation time has been associated with a lower engraftment rate [1]. Typically, the tumour fragment is cut into a size of 2–3 mm^3 and implanted in mice. Tumour growth is evaluated regularly until the tumour size reaches approximately 1000 mm^3. Then, the tumours are harvested and stored for the next stage. It takes about 3–6 months for tumour harvest [2].

PDX models reproduce the clinicopathological features of the original tumour and are used as experimental models for drug evaluation, biomarker identification, and precision medicine strategies. Current drug development has been mainly carried out using the cell line method; however, various studies have reported that drug responsiveness in the cell line methods is not sufficiently reflected in human patients [3]. The drug responsiveness in PDX models is more similar to clinically applied drug responsiveness because there are close similarities in genomic features and microenvironment status between PDX models and patient tumours [2, 4, 5]. By screening several anticancer drugs in PDX models, the most effective drug can be recommended prior to patient treatment. However, this approach is difficult because the generation of PDX models is not successful in all cases, and it takes several months to obtain the drug responsiveness data from PDX models [2]. For these reasons, a PDX cohort with genomic and drug responsiveness data has been suggested. The PDX cohort may be a powerful tool for drug development and treatment for patients with cancers [6–8]. Figure 2.1 shows a brief chart for using the PDX models. PDX models can be obtained from each type of cancer by grafting the original tumours into mice. Both the tumours of patients and the PDX models are preserved in a biobank, and several analyses have been performed, including pathological, genomic, and molecular analyses. Several anticancer drugs are evaluated using PDX models passaged from original tumours or those preserved in biobanks. These data are collected in databanks and are used for precision medicine in cancer patients in the future or for new drug development.

PDX models have been established in several cancers, including colon [9], stomach [10], breast [11], pancreas [12, 13], lung [14, 15], liver [16], kidney [17], bladder [18], uterus [8, 19–27], and ovary [28–32]; however, several questions remain unanswered. For example, what should be used as the starting material, tissue fragment, or tumour cells? Where should the materials be implanted? What is the success rate of each method? Is there any advantage or disadvantage in each method? Are there any alterations in retransplantation? This review complies with the information on the current methods of PDX in gynaecological cancers.

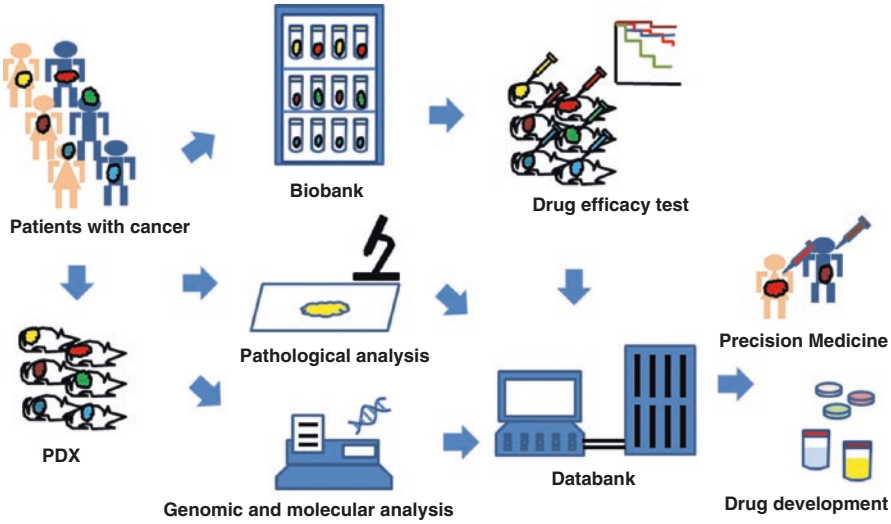

Fig. 2.1 The summary chart for using the patient-derived xenograft models. Patient-derived xenograft (PDX) models can be obtained from each cancer by grafting the original tumours into mice. These materials are preserved in biobanks and have undergone several analyses, including pathological, genomic, and molecular analysis. Several anticancer drugs are evaluated using PDX models. These data are collected in databanks and used for precision medicine for cancer patients in the future or for new drug development

2.2 Mouse Strains

The engraftment rate is important when there are limited funds and restricted specimens. It depends on several factors including the kind of recipient mice, site for implantation, method for transplantation, and size of the fragment. Nude mice, which have no thymus for mutation, were identified in 1962 by the appearance of their atrichia: they have no T cells [33]. It is easy to confirm subcutaneous engraftment since they are hairless. Severe combined immunodeficient (SCID) mice, which have no mature T and B cells due to their loss of protein kinase, DNA activated, and catalytic polypeptide (Prkdc), were identified in 1983 [34]. SCID-hu, which can be implanted in the foetal liver, thymus, and the renal capsule, contains human T cells [35]. Human T cells can increase in Hu-PBL-SCID with implanted human monocytes in their peritoneum. These mice containing human T cells contributed to the research on HIV; however, the rate and duration of implantation of human haematopoietic stem cells were unsatisfactory because SCID mice possess NK cell activity [36]. SCID–Beige is a hybrid of SCID with Beige, which has low NK cell activity; however, the rate and duration of implantation of human haematopoietic stem cells are not satisfactory [37, 38]. NOD mice have insulin-dependent diabetes mellitus (DM), where β cells in the pancreas are destroyed by T cells. They also possess low macrophage and dendritic cell activity [39]. NOD/SCID mice, which are a hybrid of NOD and SCID mice, do not show symptoms of DM because

of a deficiency of T cells; they are extremely immunodeficient [40]. NOG [41] and NSG [42] mice are hybrids of NOD/SCID with common γ-deficient mice; they do not show NK cell activity. NOG and NSG have achieved a satisfactory rate of implantation of human haematopoietic stem cells, monocytes, and malignancy. Recently, humanised mice have been used for the development of several immune checkpoint inhibitors. CD34-positive human haematopoietic stem and precursor cells were injected into NSG mice that received whole-body irradiation, resulting in reconstitution of immune cells. Humanised PDX models could be established in a partially human leukocyte antigen-matched allogeneic immune system [43–46].

2.3 Site of Transplantation

Several sites of transplantation, including subcutaneous, renal capsule, peritoneum, and orthotopic, have been reported. Subcutaneous transplantation is the most common because of the simple procedure, and it is easy to confirm the tumour implantation; however, metastasis to other organs rarely occurs (Fig. 2.2a). The minced tumour is injected subcutaneously, or the fragment of the tumour is placed subcutaneously directly after the skin is cut. The renal capsule may be used for tumours with low malignant potential or for normal tissue. The procedure is not simple; however, there is an increased blood supply for tumour growth in the renal capsule, and a high engraftment rate is expected. Mice are placed in the lateral position, and a 2-cm incision is made opposite the loin skin. The peritoneal cavity is accessed by an incision made in the abdominal wall overlying the kidney. After the kidney is exteriorised, the renal capsule and the space beneath the kidney capsule are opened. Following this, tumour fragments are inserted. Transplantation in the peritoneum is performed to examine ascites or metastasis to other organs. The minced tumour is injected into the peritoneum, or the fragment of the tumour is placed in the

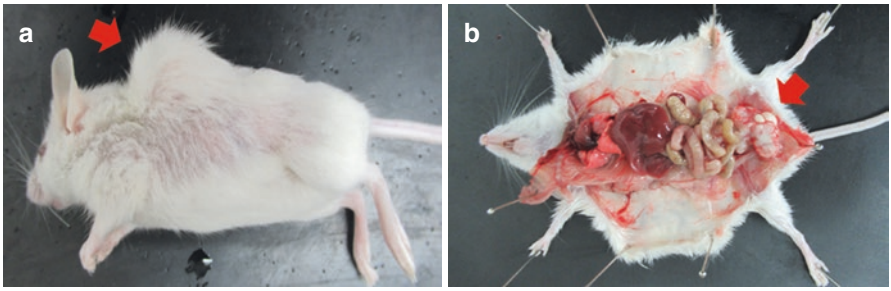

Fig. 2.2 (**a**) Subcutaneous patient-derived xenograft model. The minced tumour obtained from patients with cervical cancer were minced and injected subcutaneously into SCID mouse. After 4 months, the engrafted tumour was observed in subcutaneous layers of the mouse (red arrow). (**b**) Orthotopic patient-derived xenograft model. The minced tumour obtained from patients with cervical cancer were minced and injected into the uterine cervix of the SCID mouse transvaginally. After 4 months, the engrafted tumour was observed in the uterine cervix of the mouse (red arrow)

abdominal cavity directly below the skin cuts. The orthotopic xenograft is also common because the tumour environment can be reproduced more accurately. The minced tumour is injected into the uterus transvaginally, or the tumour fragment is placed on the primary site after the skin is cut, into the abdomen (Fig. 2.2b).

2.4 Cervical Cancer

2.4.1 PDX Procedure and Success Rate

Few reports exist on PDX models in cervical cancer. This may be a clinical feature for cervical cancer. Most patients with advanced-stage tumours receive radiotherapy or chemotherapy after biopsy. Surgical therapy may be performed at an early stage with a small lesion. Thus, it is difficult to obtain enough specimens for implantation. However, PDX models are advantageous for these patients because the tumour tissue can be expanded in mice to apply various experimental methods for tumour tissue analysis. Table 2.1 shows the previously reported literature on PDX models for cervical cancer. The engraftment rate varies from 0 to 75% [19–22]. The most important factor is probably the characteristics of each tumour, including infiltration and proliferation of each primary tumour. Hiroshima et al. implanted HER-2-positive cervical cancer, which was resected from one patient, subcutaneously and into the cervix of several nude mice with engraftment rate of 70–75% [20]. Chaudary et al. implanted a 1–2 mm tumour fragment that was resected from 33 cervical cancer patients to the cervix of SCID mice with an engraftment rate of 48%. On average, it took 3–4 months for the first palpable xenograft to arise following orthotopic transplant [21]. Hoffmann et al. implanted a 3–5 mm tumour fragment resected from six cervical cancer patients subcutaneously in SCID mice; however, no tumour engraftment was found. Then, they injected minced tumours resected from seven cervical cancer patients subcutaneously into SCID mice. The engraftment rate was approximately 70%. Palpable or visible tumours appeared 6–8 weeks after transplantation. No differences in engraftment were observed between squamous cell

Table 2.1 The engraftment rate of the patient-derived xenograft models for cervical cancer in the literature

	Mouse strains	Site of transplantation	Method of graft	Fragment size	Engraftment rate, %
Hiroshima et al.	Nude	Subcutaneous	Direct	3 mm^3	70 (7/10)
		Cervix	Direct	3 mm^3	75 (6/8)
Chaudary et al.	SCID, NOD SCID	Cervix	Direct	1–2 mm	48 (16/33)
Hoffmann et al.	SCID	Subcutaneous	Direct	3–5 mm	0 (0/6)
			Injection	Minced	70 (7/10)
Larmour et al.	NSG	Renal capsule	Direct	1 mm^3	71 (10/14)

carcinomas and adenocarcinomas [22]. Larmour et al. implanted a 1-mm^3 tumour fragment resected from 14 cervical cancer patients to the renal capsule of NSG mice with an engraftment rate of 71.4%. They also described that mouse stroma did not contribute to re-engraftment. The xenografting doses of 10^6 cells/kidney failed to generate tumours, irrespective of the presence of mouse cells. The size of the harvested xenograft limited the ability of re-engraftment. They also described that cervical dysplasia and normal tissue xenografted beneath the renal capsule could survive and grow [19].

2.4.2 Analysis of the Original Tumour and PDX

In most published literature on the PDX model of cervical cancer, there is a strong similarity of pathological findings between primary tumours and PDX. p16 overexpression, which is caused by the functional inactivation of Rb by human papillomavirus E7 protein, is peculiar in cervical cancer. Immunohistochemical findings of these proteins are also inherited from the primary tumour to PDX. Hiroshima et al. established a PDX model of HER-2-positive cervical cancer. They implanted the tumour fragment into the subcutaneous and cervix of nude mice. There were no cases of metastasis in subcutaneous PDX mice. In contrast, metastases, including peritoneal dissemination, liver, lung, and lymph node metastases, were found in the cervical orthotopic PDX model. They demonstrated that subcutaneous and cervical orthotopic xenograft tumours as well as metastases were stained by the ant-HER-2 antibody and recapitulated the histological structures of the original tumour [20]. Chaudary et al. evaluated the epithelial and stromal components of the original biopsy and xenograft models using two independent methods. The percentage of stroma tended to increase at early passages and decreased at later passages with a low value (<10%) after five passages. The decrease in stromal content in the later passage paralleled an increase in the growth rate of the tumours, as assessed by the mean time between passages. They also evaluated the epithelial and stromal components by immunostaining for SMA, collagen IV, cytokeratin, CD31, LYVE1, IFP, EF5, CA9, and Ki67. The expression of hypoxia markers (CA-9 and EF5) in the epithelial components of the tumour significantly increased with passage number. In parallel, there was a significant increase in vascular staining (CD31) in the stromal component. On average, there was also a significant increase in Ki67 staining in the epithelial component of the tumour and LYVE1 in both components. CD31 and LYVE1 levels were much lower in the epithelial component when compared to the stromal component, consistent with the finding that CA-9 and EF5 changed to a larger extent in the epithelial than in the stromal component. Ki 67 levels are much lower in the stromal component when compared to the epithelial component. A strong correlation was found between the passage 3 xenograft and primary biopsy for all markers, excluding collagen IV [21]. Larmour et al. described similar morphological features by H&E staining, and the immunostaining pattern for p16 and HPV were observed between primary tumours and several passaged xenograft

tumours. Hoffmann et al. reported that tumour markers such as EGF receptor and p16 were preserved after early and late tumour passage [19].

2.5 Endometrial Cancer

2.5.1 PDX Procedure and Success Rate

Hysterectomy is the main therapy for patients with endometrial cancer; it is easy for researchers to obtain sufficient specimens in this case. In contrast, most diseases are confined to the uterus in endometrial cancer; the prognosis does not differ in each disease. There are few studies on PDX models for endometrial cancer. Table 2.2 shows the previously reported literature on PDX models for endometrial cancer. The engraftment rate varies from 25 to 100% [8, 23–27]. Zhu et al. described PDX models using NOD/SCID mice in patients with high-risk endometrial cancer, including high-grade endometrioid carcinoma, serous carcinoma, clear cell carcinoma, and carcinosarcoma. They reported that the engraftment rate was 77.8% (14/18) regardless of the engraftment method. It was higher in the subrenal capsule models than in the subcutaneous models. The time to tumour formation varied from 2 to 11 weeks [23]. Unno et al. transplanted endometrial tumour tissue fragments to the renal capsule in NSG mice. The engraftment rate was 36.4% [24]. Depreeuw et al. reported PDX models from primary, metastatic, and recurrent type 1 and type 2 endometrial cancer patients. The engraftment rate was 60% with subcutaneous implantation using nude mice [25]. Cabrera et al. reported on PDX models from two endometrial cancers. First, they implanted tissue fragments into subcutaneous nude mice. After sufficient tumour growth, the tumours were mined and injected into the

Table 2.2 The engraftment rate of the patient-derived xenograft models for endometrial cancer in the literature

	Mouse strains	Site of transplantation	Method of graft	Fragment size	Engraftment rate, %
Zhu et al.	NOD/SCID	Renal capsule	Direct	$1 \times 1.5 \times 1.5$ mm^3	63 (16/19)
		Subcutaneous	Direct	$1 \times 1.5 \times 1.5$ mm^3	50 (9/18)
Unno et al.	NSG	Renal capsule	Direct	1.5×1.5 mm^2	36.4 (4/11)
Depreeuw et al.	Nude	Subcutaneous	Direct	8-10 mm^3	60 (24/40)
Cabrera et al.	Nude	Uterus	Injection	minced	90 (9/10)
Haldorsen et al.	NSG	Uterus	Injection	Cell suspension	100 (1/1)
Moiola et al.	Nude	Uterus	Direct	Small fragment	75–90
	Nude	Subcutaneous	Direct	5–10 mm^3	60–80
	Nude	Subcutaneous	Direct	8–10 mm^3	100
	NSG	Uterus	Injection	Cell suspension	25–100

uterus. The engraftment rate achieved was 90% and 78% of the patients that had pelvic implants [26]. Haldson et al. established patient-derived cell (PDC) models from tissues in patients with grade 3 endometrioid carcinoma. They obtained the cell suspension from the original tissue and injected them with Matrigel into the uterus of NSG mice [27]. Miola et al. described endometrial cancer PDX cohorts developed from primary tumours and metastasis covering all subtypes. In this cohort study, 124 patients with endometrial cancer were recruited from different centres across Europe. The tumour tissue fragments were implanted subcutaneously or orthotopically through a laparotomic incision into athymic nude mice. The engraftment rate of subcutaneous PDX varied from 60 to 80%; however, once the tumour was developed, the engraftment rate increased to nearly 100% in subsequent passages. It takes 3–5 months to engraft and develop the first generation. In contrast, the engraftment rate of orthotopic PDX model varied from 75 to 90% and also took 2–5 months to develop a palpable and transferable tumour. In a small study of five tumours from endometrial cancer patients, cell suspension from primary tumours with Matrigel were injected orthotopically into the uterus of NSG mice. For this type of model, the engraftment rate was lower, ranging from 25 to 100% in the first generation. Furthermore, the time of engraftment is slower; it takes an average of 10 months to develop an orthotopic PDX model [8].

2.5.2 Analysis of the Original Tumour and PDX

Zhu et al. established the endometrial cancer PDX model and evaluated the pathological and immunohistochemical features between primary tumours and PDX. No significant differences were observed among the corresponding F1 and F3 PDX with regard to architecture and cytological features, as shown by H&E. No major differences in immunohistochemical features, including hormone receptor (oestrogen receptor and progesterone receptor), the status of cytokeratin, and P53 expression were observed among the original tumours and xenograft tumours. They also validated two high-risk endometrial cancer PDXs on genomic analysis, including DNA and RNA sequencing. F0 (original) and F4 tumour DNA mutation frequencies exhibit a significant linear correlation. On RNA sequencing, the expressions of F0 and F4 tumour genes exhibited a significant linear correlation; PDX exhibited high similarity with patient rumours [23]. Unno et al. evaluated the histological and immunohistochemical features of PDX models. Serous carcinoma, carcinosarcoma, and endometrioid carcinoma xenograft tissues were stained for hormone receptors, ER and PR, the proliferation marker, Ki67, endothelial cell marker CD31, and epithelial–mesenchymal transition (EMT) markers such as cytokeratin, vimentin, E-cadherin, P53, PTEN, uPA, and uPAR. The xenografts retained the characteristics of the original tumour and displayed features that were unique to type I and type II endometrial cancer [24]. Depreeuw et al. validated the established

PDX models histologically. In all models, irrespective of their classification, the tissue architecture and the epithelial component of the original tumour by H&E staining were preserved in the corresponding F1 and F3 PDX. They observed similarities in ER and PR staining between patients and xenograft tumours. They stained tumour sections for vimentin using two different antibodies: one specific for human vimentin (hu-VIM) and a second one binding both human and mouse vimentin (hu + mo-VIM). In all patient tumours, the stroma stained positive for hu-VIM, but the staining was negative in the PDX. The hu + mo-VIM was strongly positive for xenograft stroma, indicating that the human-derived stroma was lost and replaced by a reduced amount of murine stroma after tumour engraftment in mice. They also performed whole-exome sequencing on four models reflecting a different, more common and relevant subtype of endometrial cancer, including two endometrioid, one mesonephric, and one serous carcinoma without MSI or POLE mutations. They found an average of 57 non-silent mutations in the primary tumours and 77 of them in the xenografts. The majority of such mutations were common between primary tumours and xenografts (55%), while a minor fraction was unique either for the primary tumour (11%) or for the xenograft (34%). By studying the cancer consensus genes specifically, they observed that most of the mutations were common between primary tumours and xenografts. The copy number profiles were generated using low-covered whole-genome sequencing for both the primary tumour and xenograft in the endometrioid carcinoma model. On average, 90% of the genome had the same copy number between the primary tumour and xenograft [25].

2.6 Ovarian Cancer

2.6.1 PDX Procedure and Success Rate

PDX models have been more advanced in ovarian cancer than in other gynaecological malignancies. Table 2.3 shows the engraftment rate described in recently published literature on ovarian cancer PDX models. The engraftment rate varies from 8.3 to 100% [28–32]. Wu et al. injected the minced tumour fragment dissected from ovarian cancer patients into subcutaneously into SCID mice. The engraftment rate was 15.4% [28]. Dobbin et al. evaluated the engraftment rate of ovarian cancer fragments in several implanted sites using SCID mice. The engraftment rates were 85.3% in subcutaneous, 63.6% in MFP, 22.2% in IP, and 8.3% in renal capsules [29]. Weroha et al. injected the minced ovarian cancer fragment into the intraperitoneal cavity of SCID mice. The engraftment rate was 74% [32]. Eoh et al. injected minced ovarian cancer fragment into subcutaneous NOG mice with an engraftment rate of 53.4% [30]. Heo et al. injected a small fragment of ovarian cancer in the renal capsule of nude mice. The engraftment rate was 48.8% [31].

Table 2.3 The engraftment rate of the patient-derived xenograft models for ovarian cancer in the literature

	Mouse strains	Site of transplantation	Method of graft	Fragment size	Engraftment rate, %
Wu et al.	SCID	Subcutaneous	Injection	Minced	15 (4/26)
		Ovary	Direct	3 mm^3	100 (1/1)
Dobbin et al.	SCID	Subcutaneous	Direct	5 mm^2	85
		Mammary fat pat	Direct	Minced	64
		Intraperitoneal	Injection	Minced	22
		Renal capsule	Injection	3 mm^2	8
Weroha et al.	SCID	Intraperitoneal	Injection	Minced	74
Eoh et al.	NOG	Subcutaneous	Injection	Minced	53 (47/88)
Heo et al.	Nude	Renal capsule	Direct	2–3 mm	49 (22/45)

2.6.2 Analysis of the Original Tumour and PDX

Wu et al. performed immunohistochemical analyses for primary tumours and PDX. The tumour markers, including epithelial tissue marker (CK7), intestinal tissue marker (vimentin), nervous tissue marker (Syn), tumour protein p53 (P53), proliferating cell nuclear antigen (PCNA), Antigen KI-67 (Ki67), and nuclear factor erythroid 2-like 2 (NrF2) in PDX models tumours were in accordance with primary tumours; however, immunohistochemical scores in PDX models were higher when compared to those in primary tumours. The tumour-associated gene expression of the second-generation PDX model was also in accordance with the primary tumour. They also compared gene mutation and expression between PDX model tumours and primary tumours. Single nucleotide polymorphisms (SNPs), transition, and transversion of PDX model tumours were lower when compared to those of the primary tumour; however, the location of SNPs did not differ between the groups. Fusion gene analysis indicated that compared to the primary tumour, which includes three fusion genes, there was only one fusion gene in PDX model tumours in accordance with its primary tumour. Six new fusion genes were found in PDX model tumours. The alternative splicing of PDX tumour models was lower than that of their primary tumour. The consistent rate of expressed genes reached 87.2%. These results indicated that PDX model tumours were consistent with primary tumours on gene expression [28]. Dobbin et al. performed immunohistochemistry for tumour-initiating cell markers, including ALDH1A1, CD44, and CD133. The PDX models showed similar expression of ALDH1A1 and CD133. There was a significant change in the expression of CD44; however, it decreased from 5.5% to 2.4%. Moreover, immunohistochemistry for human HLA demonstrated the replacement of human stroma with murine cells. They performed an RT^2-PCR array, which quantifies mRNA levels of 84 targetable oncogenes. Most of the 84 cancer drug target genes had similar expression in the PDX and the original patient tumour [29]. Weroha et al. reported that the glandular characteristic of adenocarcinoma was

conserved between tumourgrafts and their primary tumours. The percentage of non-epithelial tissue area, which was negative for pan-CK expression, was similar between PDX and primary tumours. When patient and tumour tissue were evaluated for the expression of human vimentin using an antibody with no reactivity against mouse protein, the patient stroma stained strongly while the tumourgraft stroma did not. Array comparative genomic hybridisation revealed a marked overlap in genomic gains and losses between the patient tumour and the corresponding tumourgraft. In addition, commonly gained/lost genes are seen in ovarian cancer. They also evaluated the efficacy of platinum-based chemotherapy. Paclitaxel–carboplatin chemotherapy reduced tumour weight in PDX models, which were grafted from patients with platinum-sensitive tumours; however, it was not observed in models that were grafted from patients with platinum-resistant tumours. The gene expression showed two distinct patterns between platinum-sensitive and platinum-resistant tumourgrafts [32]. Heo et al. reported that H&E staining of primary patient tissue and PDXs after each passage revealed a similar architectural pattern of nesting configuration and comparable cytologic atypia in PDXs according to pathologic subtype. Interestingly, they found different histologic features in PDX tissue compared with the tissue of cell line xenografts. Short tandem repeat analysis showed an almost identical banding pattern between PDXs and primary patient tumours. They also evaluated the efficacy of chemotherapy and molecular target therapy. Paclitaxel–carboplatin chemotherapy significantly decreased the tumour weight in PDX grafted from a patient with high-grade serous carcinoma, which was sensitive to paclitaxel–carboplatin chemotherapy. Moreover, the EGFR inhibitor erlotinib significantly decreased tumour weight in the PDX model grafted from a patient with clear cell carcinoma, which strongly expressed EGFR [31].

2.7 Conclusions

Several aspects of human patient tumour tissue, including genomic and histological characteristics or sensitivity of anticancer drugs, are preserved in PDX models. These advantages could bring about drug development and appropriate treatment for precision medicine. PDX models are indispensable tools for precision oncology today.

References

1. Guerrera F, Tabbò F, Bessone L, Maletta F, Gaudiano M, Ercole E, et al. The influence of tissue ischemia time on RNA integrity and patient-derived xenografts (PDX) engraftment rate in a non-small cell lung cancer (NSCLC) biobank. PLoS One. 2016;11(1):e0145100. https://doi.org/10.1371/journal.pone.0145100.
2. Cho SY, Kang W, Han JY, Min S, Kang J, Lee A, et al. An integrative approach to precision cancer medicine using patient-derived xenografts. Mol Cells. 2016;39(2):77–86. https://doi.org/10.14348/molcells.2016.2350.

3. Wilding JL, Bodmer WF. Cancer cell lines for drug discovery and development. Cancer Res. 2014;74(9):2377–84. https://doi.org/10.1158/0008-5472.can-13-2971.
4. Rosfjord E, Lucas J, Li G, Gerber HP. Advances in patient-derived tumor xenografts: from target identification to predicting clinical response rates in oncology. Biochem Pharmacol. 2014;91(2):135–43. https://doi.org/10.1016/j.bcp.2014.06.008.
5. Hidalgo M, Bruckheimer E, Rajeshkumar NV, Garrido-Laguna I, De Oliveira E, Rubio-Viqueira B, et al. A pilot clinical study of treatment guided by personalized tumorgrafts in patients with advanced cancer. Mol Cancer Ther. 2011;10(8):1311–6. https://doi.org/10.1158/1535-7163.mct-11-0233.
6. Gao H, Korn JM, Ferretti S, Monahan JE, Wang Y, Singh M, et al. High-throughput screening using patient-derived tumor xenografts to predict clinical trial drug response. Nat Med. 2015;21(11):1318–25. https://doi.org/10.1038/nm.3954.
7. Byrne AT, Alférez DG, Amant F, Annibali D, Arribas J, Biankin AV, et al. Interrogating open issues in cancer precision medicine with patient-derived xenografts. Nat Rev Cancer. 2017;17(4):254–68. https://doi.org/10.1038/nrc.2016.140.
8. Moiola CP, Lopez-Gil C, Cabrera S, Garcia A, Van Nyen T, Annibali D, et al. Patient-derived xenograft models for endometrial cancer research. Int J Mol Sci. 2018;19(8):2431. https://doi.org/10.3390/ijms19082431.
9. Aytes A, Molleví DG, Martinez-Iniesta M, Nadal M, Vidal A, Morales A, et al. Stromal interaction molecule 2 (STIM2) is frequently overexpressed in colorectal tumors and confers a tumor cell growth suppressor phenotype. Mol Carcinog. 2012;51(9):746–53. https://doi.org/10.1002/mc.20843.
10. Choi YY, Lee JE, Kim H, Sim MH, Kim KK, Lee G, et al. Establishment and characterisation of patient-derived xenografts as paraclinical models for gastric cancer. Sci Rep. 2016;6:22172. https://doi.org/10.1038/srep22172.
11. Zhang X, Claerhout S, Prat A, Dobrolecki LE, Petrovic I, Lai Q, et al. A renewable tissue resource of phenotypically stable, biologically and ethnically diverse, patient-derived human breast cancer xenograft models. Cancer Res. 2013;73(15):4885–97. https://doi.org/10.1158/0008-5472.can-12-4081.
12. Chen Q, Wei T, Wang J, Zhang Q, Li J, Zhang J, et al. Patient-derived xenograft model engraftment predicts poor prognosis after surgery in patients with pancreatic cancer. Pancreatology. 2020;20(3):485–92. https://doi.org/10.1016/j.pan.2020.02.008.
13. Mattie M, Christensen A, Chang MS, Yeh W, Said S, Shostak Y, et al. Molecular characterization of patient-derived human pancreatic tumor xenograft models for preclinical and translational development of cancer therapeutics. Neoplasia (New York, NY). 2013;15(10):1138–50. https://doi.org/10.1593/neo.13922.
14. Lee HW, Lee JI, Lee SJ, Cho HJ, Song HJ, Jeong DE, et al. Patient-derived xenografts from non-small cell lung cancer brain metastases are valuable translational platforms for the development of personalized targeted therapy. Clin Cancer Res. 2015;21(5):1172–82. https://doi.org/10.1158/1078-0432.ccr-14-1589.
15. Dong X, Guan J, English JC, Flint J, Yee J, Evans K, et al. Patient-derived first generation xenografts of non-small cell lung cancers: promising tools for predicting drug responses for personalized chemotherapy. Clin Cancer Res. 2010;16(5):1442–51. https://doi.org/10.1158/1078-0432.ccr-09-2878.
16. Zhu M, Li L, Lu T, Yoo H, Zhu J, Gopal P, et al. Uncovering biological factors that regulate hepatocellular carcinoma growth using patient derived xenograft assays. Hepatology (Baltimore, MD). 2020; https://doi.org/10.1002/hep.31096.
17. Sivanand S, Peña-Llopis S, Zhao H, Kucejova B, Spence P, Pavia-Jimenez A, et al. A validated tumorgraft model reveals activity of dovitinib against renal cell carcinoma. Sci Transl Med. 2012;4(137):137ra75. https://doi.org/10.1126/scitranslmed.3003643.
18. Park B, Jeong BC, Choi YL, Kwon GY, Lim JE, Seo SI, et al. Development and characterization of a bladder cancer xenograft model using patient-derived tumor tissue. Cancer Sci. 2013;104(5):631–8. https://doi.org/10.1111/cas.12123.

19. Larmour LI, Cousins FL, Teague JA, Deane JA, Jobling TW, Gargett CE. A patient derived xenograft model of cervical cancer and cervical dysplasia. PLoS One. 2018;13(10):e0206539. https://doi.org/10.1371/journal.pone.0206539.
20. Hiroshima Y, Zhang Y, Zhang N, Maawy A, Mii S, Yamamoto M, et al. Establishment of a patient-derived orthotopic Xenograft (PDOX) model of HER-2-positive cervical cancer expressing the clinical metastatic pattern. PLoS One. 2015;10(2):e0117417. https://doi.org/10.1371/journal.pone.0117417.
21. Chaudary N, Pintilie M, Schwock J, Dhani N, Clarke B, Milosevic M, et al. Characterization of the tumor-microenvironment in patient-derived cervix xenografts (OCICx). Cancers. 2012;4(3):821–45. https://doi.org/10.3390/cancers4030821.
22. Hoffmann C, Bachran C, Stanke J, Elezkurtaj S, Kaufmann AM, Fuchs H, et al. Creation and characterization of a xenograft model for human cervical cancer. Gynecol Oncol. 2010;118(1):76–80. https://doi.org/10.1016/j.ygyno.2010.03.019.
23. Zhu M, Jia N, Nie Y, Chen J, Jiang Y, Lv T, et al. Establishment of patient-derived tumor xenograft models of high-risk endometrial cancer. Int J Gynecol Cancer. 2018;28(9):1812–20. https://doi.org/10.1097/igc.0000000000001365.
24. Unno K, Ono M, Winder AD, Maniar KP, Paintal AS, Yu Y, et al. Establishment of human patient-derived endometrial cancer xenografts in NOD scid gamma mice for the study of invasion and metastasis. PLoS One. 2014;9(12):e116064. https://doi.org/10.1371/journal.pone.0116064.
25. Depreeuw J, Hermans E, Schrauwen S, Annibali D, Coenegrachts L, Thomas D, et al. Characterization of patient-derived tumor xenograft models of endometrial cancer for preclinical evaluation of targeted therapies. Gynecol Oncol. 2015;139(1):118–26. https://doi.org/10.1016/j.ygyno.2015.07.104.
26. Cabrera S, Llauradó M, Castellví J, Fernandez Y, Alameda F, Colás E, et al. Generation and characterization of orthotopic murine models for endometrial cancer. Clin Exp Metastasis. 2012;29(3):217–27. https://doi.org/10.1007/s10585-011-9444-2.
27. Haldorsen IS, Popa M, Fonnes T, Brekke N, Kopperud R, Visser NC, et al. Multimodal imaging of orthotopic mouse model of endometrial carcinoma. PLoS One. 2015;10(8):e0135220. https://doi.org/10.1371/journal.pone.0135220.
28. Wu J, Zheng Y, Tian Q, Yao M, Yi X. Establishment of patient-derived xenograft model in ovarian cancer and its influence factors analysis. J Obstet Gynaecol Res. 2019;45(10):2062–73. https://doi.org/10.1111/jog.14054.
29. Dobbin ZC, Katre AA, Steg AD, Erickson BK, Shah MM, Alvarez RD, et al. Using heterogeneity of the patient-derived xenograft model to identify the chemoresistant population in ovarian cancer. Oncotarget. 2014;5(18):8750–64. https://doi.org/10.18632/oncotarget.2373.
30. Eoh KJ, Chung YS, Lee SH, Park SA, Kim HJ, Yang W, et al. Comparison of clinical features and outcomes in epithelial ovarian cancer according to tumorigenicity in patient-derived xenograft models. Cancer Res Treat. 2018;50(3):956–63. https://doi.org/10.4143/crt.2017.181.
31. Heo EJ, Cho YJ, Cho WC, Hong JE, Jeon HK, Oh DY, et al. Patient-derived xenograft models of epithelial ovarian cancer for preclinical studies. Cancer Res Treat. 2017;49(4):915–26. https://doi.org/10.4143/crt.2016.322.
32. Weroha SJ, Becker MA, Enderica-Gonzalez S, Harrington SC, Oberg AL, Maurer MJ, et al. Tumorgrafts as in vivo surrogates for women with ovarian cancer. Clin Cancer Res. 2014;20(5):1288–97. https://doi.org/10.1158/1078-0432.ccr-13-2611.
33. Flanagan SP. 'Nude', a new hairless gene with pleiotropic effects in the mouse. Genet Res. 1966;8(3):295–309. https://doi.org/10.1017/s0016672300010168.
34. Bosma GC, Custer RP, Bosma MJ. A severe combined immunodeficiency mutation in the mouse. Nature. 1983;301(5900):527–30. https://doi.org/10.1038/301527a0.
35. McCune JM, Namikawa R, Kaneshima H, Shultz LD, Lieberman M, Weissman IL. The SCID-hu mouse: murine model for the analysis of human hematolymphoid differentiation and function. Science (New York, NY). 1988;241(4873):1632–9. https://doi.org/10.1126/science.2971269.

36. Mosier DE, Gulizia RJ, Baird SM, Wilson DB. Transfer of a functional human immune system to mice with severe combined immunodeficiency. Nature. 1988;335(6187):256–9. https://doi.org/10.1038/335256a0.
37. Thomsen M, Galvani S, Canivet C, Kamar N, Böhler T. Reconstitution of immunodeficient SCID/beige mice with human cells: applications in preclinical studies. Toxicology. 2008;246(1):18–23. https://doi.org/10.1016/j.tox.2007.10.017.
38. Mosier DE, Stell KL, Gulizia RJ, Torbett BE, Gilmore GL. Homozygous scid/scid;beige/beige mice have low levels of spontaneous or neonatal T cell-induced B cell generation. J Exp Med. 1993;177(1):191–4. https://doi.org/10.1084/jem.177.1.191.
39. Kikutani H, Makino S. The murine autoimmune diabetes model: NOD and related strains. Adv Immunol. 1992;51:285–322. https://doi.org/10.1016/s0065-2776(08)60490-3.
40. Gerling IC, Serreze DV, Christianson SW, Leiter EH. Intrathymic islet cell transplantation reduces beta-cell autoimmunity and prevents diabetes in NOD/Lt mice. Diabetes. 1992;41(12):1672–6. https://doi.org/10.2337/diab.41.12.1672.
41. Ito M, Hiramatsu H, Kobayashi K, Suzue K, Kawahata M, Hioki K, et al. NOD/SCID/gamma(c)(null) mouse: an excellent recipient mouse model for engraftment of human cells. Blood. 2002;100(9):3175–82. https://doi.org/10.1182/blood-2001-12-0207.
42. Shultz LD, Lyons BL, Burzenski LM, Gott B, Chen X, Chaleff S, et al. Human lymphoid and myeloid cell development in NOD/LtSz-scid IL2R gamma null mice engrafted with mobilized human hemopoietic stem cells. J Immunol (Baltimore, Md: 1950). 2005;174(10):6477–89. https://doi.org/10.4049/jimmunol.174.10.6477.
43. Morton JJ, Bird G, Refaeli Y, Jimeno A. Humanized mouse xenograft models: narrowing the tumor-microenvironment gap. Cancer Res. 2016;76(21):6153–8. https://doi.org/10.1158/0008-5472.can-16-1260.
44. Wang M, Yao LC, Cheng M, Cai D, Martinek J, Pan CX, et al. Humanized mice in studying efficacy and mechanisms of PD-1-targeted cancer immunotherapy. FASEB J. 2018;32(3):1537–49. https://doi.org/10.1096/fj.201700740R.
45. Rongvaux A, Willinger T, Martinek J, Strowig T, Gearty SV, Teichmann LL, et al. Development and function of human innate immune cells in a humanized mouse model. Nat Biotechnol. 2014;32(4):364–72. https://doi.org/10.1038/nbt.2858.
46. Wunderlich M, Chou FS, Link KA, Mizukawa B, Perry RL, Carroll M, et al. AML xenograft efficiency is significantly improved in NOD/SCID-IL2RG mice constitutively expressing human SCF, GM-CSF and IL-3. Leukemia. 2010;24(10):1785–8. https://doi.org/10.1038/leu.2010.158.